Journal Name

RSCPublishing

ARTICLE

Cite this: DOI: 10.1039/x0xx00000x

Received 00th January 2012,
Accepted 00th January 2012

DOI: 10.1039/x0xx00000x

www.rsc.org/

Oxidation of a model alkane aerosol by OH radical: the emergent nature of reactive uptake

F. A. Houle[a]*, W. D. Hinsberg[b], and K. R. Wilson[a]*,

An accurate description of the evolution of organic aerosol in the Earth's atmosphere is essential for climate models. However, the complexity of multiphase chemical and physical transformations has been challenging to describe at the level required to predict aerosol lifetimes and changes in chemical composition. In this work a model is presented that reproduces experimental data for the early stages of oxidative aging of squalane aerosol by hydroxyl radical (OH), a process governed by reactive uptake of gas phase species onto the particle surface. Simulations coupling free radical reactions and Fickian diffusion are used to elucidate how the measured uptake coefficient reflects the elementary steps of sticking of OH to the aerosol as a result of a gas-surface collision, followed by very rapid abstraction of hydrogen and subsequent free radical reactions. It is found that the uptake coefficient is not equivalent to a sticking coefficient or an accommodation coefficient: it is an intrinsically emergent process that depends upon particle size, viscosity, and OH concentration. An expression is derived to examine how these factors control reactive uptake over a broad range of atmospheric and laboratory conditions, and is shown to be consistent with simulation results. Well-mixed, liquid behavior is found to depend on the reaction conditions in addition to the nature of the organic species in the aerosol particle.

1. Introduction

The quantity and chemical composition of sub-micron particles (i.e. aerosols) play an important role in the Earth's climate system by directly scattering or absorbing incoming solar radiation and by indirectly modifying cloud properties. Atmospheric aerosols are comprised of inorganic salts and complex mixtures of organic molecules whose transformations involve both chemical composition (e.g. reactive uptake of gases) and the physical state (e.g. non-reactive uptake) of the aerosol. The volatility and viscosity of the aerosols' components as well as their water content, which can dynamically modify viscosity, are identified as key characteristics.[1] Current atmospheric models parameterize organic aerosol formation and evolution using equilibrium partitioning theory,[2] which assumes that molecules within the aerosol are well-mixed and respond rapidly to atmospheric conditions. In this context, well-mixed means behavior consistent with complete compositional uniformity. Recent studies[3-6] suggest that some organic aerosols exist in a glassy or semisolid phase, which can significantly affect the rates and mechanisms of the uptake of water[7, 8] and other gas phase species as well as heterogeneous oxidation chemistry.[1]

Laboratory studies of model systems are essential to unravel these factors and provide a rigorous foundation for climate model parameters. Significant focus has been placed on heterogeneous reactions of OH with various organic aerosols,[8-16] especially the determination of uptake coefficients (γ). These coefficients connect the gas composition of the atmosphere to the total extent of conversion of a chemical species to products in an aerosol per collision with a gas phase reagent. For the case where the uptake coefficient is quantified by measuring the reactive decay of an aerosol phase species,

$$\gamma = \frac{2 k_{rx} D_p \rho_0 N_A}{3 c M} \quad (1)$$

where k_{rx} is the second order heterogeneous reaction coefficient between the oxidant and the organic aerosol, D_p, is the diameter of the aerosol particle, ρ_0 is the particle's density, NA is Avogadro's number, c is the mean velocity of the gaseous oxidant, and M is the molecular weight of the organic species in the particle. It should be noted that the observed k_{rx} (unlike a gas phase bimolecular rate coefficient) depends upon the particle surface area. γ includes a geometric factor so is a more useful means of comparing reactivity in a geometry-

independent way than k_{rx}. This expression explicitly assumes that the aerosol particle is well-mixed on the timescale of the reaction.[16]

γ combines initial surface and bulk accommodation and reaction of the oxidant with subsequent chain reaction steps into a single quantity, which makes the separation of gas accommodation from a chemical reaction difficult.[17] Significant thought has been put into the nature of accommodation in gas-aerosol interactions. Because it is this specific physical process that is the subject of this paper, a set of definitions is presented in Table 1.

Table 1. Terminology for gas-aerosol interactions

Term	Definition
Thermal Accommodation[a]	The process of a gas species coming into thermal equilibrium with a surface during a gas-surface collision, α_t
Surface Accommodation[a]	Surface adsorption or trapping as a result of a gas-surface collision, held by weak interactions. Other term: physisorption. β
Bulk Accommodation[a]	Incorporation of gas into the sub-surface region of a particle following surface accommodation. This involves mass transport, α_b
Sticking Coefficient	Microscopic step involving surface adsorption or trapping as a result of a gas-surface collision, held by chemical bonds or weak interactions. Other terms: physisorption or chemisorption. α
Accommodation	General term meaning gas adsorption and absorption, α

[a] Definitions are taken from Reference[17]

These terms differentiate between various subtleties associated with capturing of a gas molecule by a particle. From a microscopic step perspective, the term accommodation only covers one kind of gas-surface interaction, leading to weakly bound adsorbates that can subsequently desorb or react to form specific chemical products. Although intended to be general, it does not fully capture situations such as a collision to form a surface species that can be either strongly or weakly bound, perhaps interconverting between these states to diffuse on the surface, and eventually react either on the surface or beneath it, or desorb. Species such as OH have both an unpaired electron and a hydrogen that will lead to complex and evolving interactions. OH collisions with an initially aliphatic surface that progressively oxidizes and adds sites for hydrogen bonding, followed by rapid reactions, are likely not to fit neatly into a surface accommodation picture at the microscopic level. Indeed, scattering of hyperthermal OH from squalane has shown that there is a sufficiently strong interaction potential between the radical and the aliphatic liquid to provide a torque to the OH molecule, resulting in significant rotational excitation.[18] Because the overall goal of our research program is to develop a detailed, microscopic chemical description of gas-aerosol interactions and aerosol aging for comparison to experiments, in this work we use the term *sticking coefficient* to measure the net probability that a gas striking a particle surface will remain there for a sufficient time to undergo chemical reaction, i.e. the fraction of incident gas molecules that are not elastically or inelastically scattered, and do not redesorb without reaction. This definition does not carry any particular assumptions about the nature of the molecule-particle interaction, which is not sufficiently characterized in this system to be described in specific detail. Because the term accommodation is accepted and understood in the literature, we also use it in this paper to describe the surface adsorption - bulk absorption processes associated with gas uptake. It is not equivalent to sticking as defined above.

If an uptake coefficient is measured by disappearance of the gas reactant, and the probability for a gas to become adsorbed or absorbed is 1, then its maximum value is 1. If the uptake coefficient is measured by disappearance of the aerosol component, then it can be larger than 1, which is interpreted to mean that a free radical chain reaction is involved in the transformation of the aerosol.[19, 20] Values less than 1 are ambiguous, reflecting the accommodation process as the only rate determining step, or alternatively a combination of accommodation and reaction. Typical values for the uptake of OH by saturated organic compounds are 0.3-1.0.[11, 12, 16, 20, 21] Because the primary reaction between OH and a hydrocarbon is the abstraction of an H atom, a very fast process, γ in this chemical system has been interpreted to mean that OH accommodates efficiently, i.e. nearly every OH collision results in an oxidation reaction, and therefore γ represents the overall accommodation process directly.

A more refined interpretation of experimentally determined uptake coefficients is made using kinetic models that represent elementary properties of the chemical reactions such as gas sticking, gas desorption, bulk diffusion, and elementary reaction steps. The models range from analytical expressions for uptake coefficients linking gas-particle reactions to measured rates of disappearance of the starting material in the aerosols, to coupled resistor schemes that treat competing processes as a set of independent paths having first order rate laws,[22] to comprehensive treatments of reaction-diffusion processes using coupled differential equation integration to generate spatially resolved concentration vs time dependences.[23] Each of these approaches is valuable for analysis of experimental results, however each involves specific approximations that must be considered when comparing the modeling results to observations. The resistor model separates accommodation and gas transport from chemical reactions on and in an aerosol, but the elementary reaction steps are not described in detail. Comprehensive microscopic models that couple reaction and transport enable an internal view of the transformation of a particle with time as oxidation progresses.[24-29] This more detailed treatment has significantly broadened thinking about the complexity of aerosol transformations, but many of the required rate constants have not been measured. Additionally, diffusion is treated with a constant average rate initially determined from Fickian kinetics but not dynamically varied as local concentration gradients change throughout the oxidation process, leading to variances from the actual rates, and the oxidation reactions are simplified to include only general steps rather than the detailed free radical chains that are proposed to occur.

In order to refine the current understanding of the aerosol oxidation process and the meaning of γ, we report new kinetic simulations of reaction-diffusion processes for a specific well-characterized heterogeneous reaction, OH + squalane (γ = 0.26, the value before the gas phase OH diffusion correction, a factor of about 10%, is applied).[16, 30-32] Specific modeling of gas phase diffusion, which has a small kinetic effect for the conditions studied,[16] is neglected for

simplicity. The computational methods used provide a straightforward way to add a full gas phase description whenever it is required for systems where the aerosol particle acts as a local sink for reactants. We include time-varying gradient driven diffusion and a more explicit description of the chemical reaction steps, and use stochastic methods instead of integration to solve the master equation for the coupled reaction-diffusion system. Since this method enables generation of an absolute time base, the kinetic model is directly validated using experimental data. The simulation results are used to consider the interpretation of γ in detail, revealing that the currently accepted definition carries some key assumptions about the reacting system that have not been previously recognized. We propose a more general expression for γ that enables a closer connection to be drawn between the disappearance of the starting material in an organic aerosol and the underlying gas-particle interactions and reaction processes.

2. Simulation methods

Stochastic algorithms for Markov processes, embodied in the Kinetiscope© software package used this study, (based on open access codes[33]) were developed in the 1970s to address systems not well-modeled deterministically.[34, 35] The algorithms are a subclass of kinetic Monte Carlo simulations, executing a random walk through event space, where an event is an individual reaction or diffusion step, rather than physical space, to generate a fully accurate time history of the system. They are exceptionally versatile, and have been extended over the years to accommodate key processes in materials chemistry such as dynamic volume changes, rare events controlled by coupled equilibria[36, 37] and coupled reaction-diffusion processes.[38] Reactions in spatially inhomogeneous systems are simulated using a set of compartments of suitable (and not necessarily uniform) size, each of which is internally instantaneously mixed and reacts according to the specific set of mechanistic steps assigned to it. These steps can vary from compartment to compartment according to local composition. Diffusion of species between the compartments follows the appropriate Fickian kinetics, either type I (as used in this work) or type II, and the individual rates are updated every time a local concentration changes due to reaction. Reaction steps and diffusion steps are treated together as a single mechanism in the algorithm that propagates the simulation. [38] In prior work we have used simulations to extract fundamental rate constants for chemical steps, and for reaction mechanism validation.[39] These studies have led to a number of new insights about the characteristics of reactions in complex condensed phase systems.[40, 41] Previous generations of Kinetiscope© are described in the references.

3. Construction of the Model and Simulation Results

In this study we define a mechanism that is as simple as possible yet captures relevant details. This enables a focus on studying the distinction between sticking and overall reaction during the uptake process. In other work we examine the free radical reactions in greater detail.[42] The reaction of OH with squalane (RH), a $C_{30}H_{62}$ branched alkane, is initiated by H atom abstraction step leading to formation of water and an alkyl free radical (R·).

$$RH + OH \rightarrow R\cdot + H_2O \quad (2)$$

Water evaporates quickly from the particle, leaving behind only small amounts in the hydrophobic environment. The alkyl radical rapidly reacts with O_2 either from the gas phase or dissolved in the particle to form a peroxy radical ($RO_2\cdot$).

$$R\cdot + O_2 \rightarrow RO_2\cdot \quad (3)$$

This species is relatively unreactive and accumulates until second order reactions become kinetically significant,

$$RO_2\cdot + RO_2\cdot \rightarrow \text{Stable Products} + O_2 \quad (4)$$

leading to the formation of stable ketone and/or alcohol products (via the Russell and/or Bennett Summers mechanisms).[43, 44] The oxidation reaction is usually written as a more complex scheme[20] but simulations show that under the conditions accessed in the experiments[16] only the reactions in Eqs. 2-4 are active. This scheme is only valid up to about 3-4 generations of oxidation, beyond which C-C bond scission reactions (i.e. fragmentation) begin to compete successfully with ketone and alcohol formation.[30, 31]

Observations suggest that a squalane particle is well mixed on the timescale of the reaction with OH.[16, 31] This enables the mechanism to be used to calculate reaction product distributions as a function of time in two ways in order to probe mixing as well as chemistry: first, by representing the particle as a single instantaneously mixed object or compartment and second, by fully coupled reaction-diffusion simulations. A diameter of 160 nm was used to replicate the average diameter used in the experiments.[16] The reaction steps and rate constants are shown in Table 2. For simplicity we use a generic set of rate constants, this is not expected to be a drastic approximation because the chemical mechanism is not very detailed. While the adsorption rate constant is based on a gas phase value, reasonable for a surface-located step, the free radical reactions use condensed phase rate constants. In a separate study we

Table 2. Reaction scheme, rate constants and diffusion coefficients used in full coupled reaction-diffusion simulations.

Reaction Step	Rate Constant	Notes
$OH + site \rightarrow OH_{ads}$	1×10^{10} cm^3/molec-s[45]	a
$OH_{ads} + RH(n) \rightarrow R\cdot(n) + H_2O$ (n=0-4)	1.55×10^{-11} cm^3/molec-s[46]	b
$O_2 + R\cdot(n) \rightarrow RO_2\cdot(n)$ (n=0-4)	2.5×10^{-12} cm^3/molec-s[46]	b,c
$RO_2\cdot(n) + RO_2\cdot(m) \rightarrow RH(n+1) + RH(m+1)$ (n,m = 0-4)	4×10^{-15} cm^3/molec-s[46]	b
$D_{Squalane}$	8.5×10^{-7} cm^2/s[47]	
D_{OH}	1×10^{-4} cm^2/s[48]	

[a] site is an adsorption site on the surface of the particle, one per squalane in the top 1 nm thick compartment. The rate coefficient applies to aliphatic molecules with a viscosity similar to squalane (see discussion section). This step was merged with the abstraction step for single compartment calculations.

[b] RH(0) = squalane. The stable oxidation products are denoted as RH(1) = SqO , RH(2) = SqO2, RH(3) = SqO3. Analogous notation is

used to describe generations of free radicals derived from squalane and its stable oxidation products.

[c] O2 concentration in the particle is assumed to be at Henry's law solubility, H_2O = 0.18 (kH,cc, the dimensionless ratio).[19, 49]

examine the detailed mechanism over 10 generations of oxidation, and will extend the present work to include it.[42] The single instantaneously mixed compartment and full reaction-diffusion simulations use the same reactions except for the explicit sticking step. In the single compartment the gas sticking and H abstraction steps are combined using the experimentally determined uptake coefficient γ and its associated rate constant k_{rx}, 1.28 x 10^{-12} cm^3/molec-s for a 160 nm diameter particle.[16] k_{rx} is obtained from phenomenological fit to the disappearance curve for the organic starting material in the aerosol particle and is proportional to γ. The fitting process does not take into account the finite surface area of the aerosol particle, so the resulting k_{rx} depends upon particle size.[50, 51]

The mechanism in Table 2 focuses on disappearance of squalane as a result of reaction with OH through several generations, not on the detailed product distributions determined experimentally.[32] Combined oxidation generations are tracked using RH(n), where n denotes the number of oxygenated functional groups added to the squalane carbon backbone to form ketones or alcohols. The H-abstraction rate constant for primary, secondary and tertiary hydrogens is assumed to be a single average value for all oxidation generations. Single values were also assumed for all secondary reaction steps.[16, 19] Oxygen is taken to be at its Henry's law saturation concentration in the particle at all times, and was not explicitly modeled.[19]

3.1 The particle modeled as a single instantaneously mixed compartment

The reaction scheme in Table 2 is evaluated by comparing experimental data obtained by reacting squalane aerosol particles for 37 seconds with OH, whose gas density ranges from 5 x 10^{10} to 5 x 10^{11} molec/cm^3, to results of single compartment simulations performed using a mid-range value of 1 x 10^{11} molec/cm^3. It has been found experimentally that product distributions vary only with total exposure of squalane to OH in the flow tube, not with partial pressure, enabling overlay of measurements taken over a range of pressures to be collected into a single data set presented in Figure 1.[16] The units of the abscissa are interchangeable with time at a given partial pressure. Thus, simulation results calculated for a single OH density yield concentration *vs* time curves that can be directly compared to experiment. The kinetic evolution of the oxidized product generations (SqOn) are found to be in excellent agreement with the experimental data[16] for 3 oxidized generations with no adjustable parameters, as shown in Figure 1. This supports the previous interpretation of the experimental data in terms of progressive oxidation of a well-mixed liquid droplet.[16, 31]

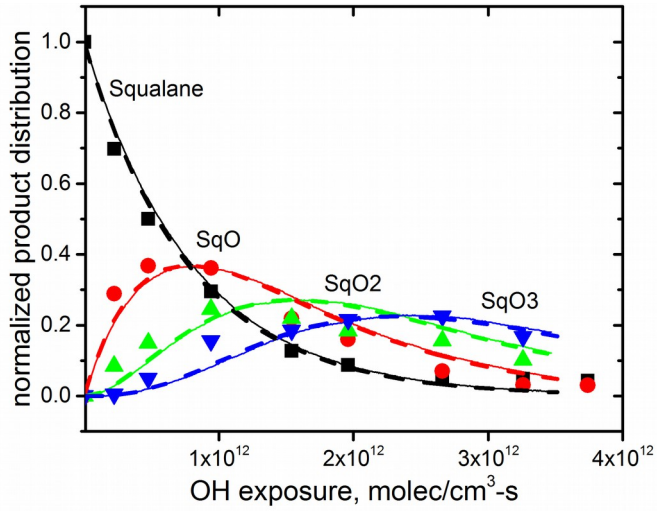

Figure 1. Overlay of experimental measurements of squalane, SqO, SqO_2 and SqO_3, the total oxidation product concentrations for the first through third oxidation generations (symbols), with simulation results. The data were measured for a single particle size, 160 nm, over an OH density range of 5 x 10^{10} to 5 x 10^{11} molec/cm^3 at an average temperature of 35 □C.[16] The viscosity of squalane is about 18 mPa-s at this temperature.[52] Simulations represented the particle as a single compartment (dashed lines) or as a set of layers coupled by diffusion (solid lines). At a mid-range OH density of 1x10^{11} molec/cm^3, the abscissa scale corresponds to a time span of 0 to 40 seconds.

3.2 Reaction-diffusion model of aerosol oxidation

The scheme is used in a full reaction-diffusion simulation in order to evaluate the role of diffusion and examine the location of very fast events such as H abstraction. The geometry is a column of layers each 80 x 80 x 1 nm^3, forming a stack of 80 compartments spanning the center of the particle to the outer surface. Cartesian coordinates are used rather than spherical, so the outer surface compartments do not strictly map onto the surface of the particle. This approximation has been evaluated by changing the size of the compartments, and the results of the simulations are found to be independent of the compartment area, but not of compartment thickness. A value of 1 nm is found to give a close representation of a continuous liquid.

The adsorption, abstraction and transport steps, captured implicitly in the single instantaneously mixed compartment model, are described explicitly. Impinging OH is allowed to stick to any squalane molecule (a site in Table 2) in the top compartment, and react with a squalane in a separate elementary step. We use the term sticking instead of accommodation as defined in Table 1 because sticking does not carry an underlying assumption about the nature of the gas-aerosol interaction.[17] The simulations in this work are performed at the level of specific chemical reactions rather than overall disappearance of squalane. A surface science description treats sticking as a gas-surface interaction that leads to a kinetically significant residence time on the surface. The details of the sticking process are not defined, but according to OH collision dynamics studies with an aliphatic surface[53] an Eley-Rideal mechanism, which involves prompt, direct interactions between the gas and the molecule it collides with, could be appropriate. The interaction between more heavily oxidized aerosol and OH is more consistent with Langmuir-Hinshelwood kinetics however, indicating that longer residence times could become important when hydrogen-bonding sites are

available.[54] These longer times may or may not be reflected in the initial sticking dynamics, and theoretical studies to elucidate the adsorption physics and understand the factors affecting OH surface lifetime would be very valuable. Because sticking is separate from reaction, an H abstraction rate constant k_{abs} typical of gas phase values[45] for secondary H abstraction in larger alkanes is used instead of the experimentally derived k_{rx} which is phenomenologically tied to the uptake coefficient and to the particle size.

The molecular components in each individual compartment are instantaneously mixed, and reactants and products are all allowed to diffuse freely between compartments according to their continuously updated concentration gradients using a standard Fickian rate law. The diffusion coefficient for OH in alkanes is assumed to be similar to diffusion of water, and an upper limit in the observed range was used because OH is smaller.[48] The self-diffusion coefficient of squalane has been determined experimentally.[47] All of the reaction products are assumed to have a self-diffusion coefficient identical to that of squalane and remain constant throughout the evolution of a pure material to a mixture. This is likely an oversimplification in general, but not anticipated to be an important one for the early stages of oxidation.

Since the adsorption rate constant for OH on squalane surfaces (k') has not been directly measured we estimate it from gas kinetics. The pseudo-first order $k' = \gamma[OH]_g cA/4$, where the experimental uptake coefficient γ is assumed to be the same as a sticking coefficient as defined in Table 1, A is the surface area of the top surface of the simulated system, over which squalane diffuses freely and therefore is available everywhere for adsorption. For an OH concentration of 1 x 10^{11} molec/cm^3 and γ = 0.26 (i.e. the experimental value), k' is computed to be 2.6 x 10^4 sec^{-1}. Using this value, the simulation results do not reproduce the experimental data: instead of squalane being consumed on a timescale of 37s as shown in Figure 1, it disappears in about 0.02 sec.

Because equating γ with a sticking coefficient does not yield a rate constant that is consistent with experimental observations, we sought to find a better value for k' by treating it as an adjustable parameter, the only one in the model. We varied k' until the observed time scale for squalane consumption was obtained. The results, essentially indistinguishable from a single compartment simulation, are shown in Figure 1. The best fit value of k'= 10 s^{-1} indicates that the uptake coefficient γ as determined from the experimental measurements is not equivalent to a sticking coefficient as conceptualized in this work, or an accommodation coefficient as is more generally used in the aerosol literature, even in this fast-reacting system. Since the rate constant expression for k' reflects the gas kinetics in the system, we can calculate a sticking coefficient from it using the best fit value for k' from the simulations. By replacing γ in the equation for k' with an elementary sticking coefficient σ, we estimate σ to be 10^{-4}. This is the same order of magnitude as the measured uptake coefficient for OH and O(^{3}P) on unreactive halocarbon surfaces,[8, 55-57] but much less than the experimental γ for squalane, or 1. γ is measured using disappearance curves for squalane as a function of time at various OH densities and reflects a combination of sticking of OH and subsequent reactions. Our finding that sticking is inefficient indicates that the value for γ in this system is reflective of the post-adsorption reaction mechanism rather than the sticking event.

In the single compartment, instantaneously mixed system, all squalane molecules are available for reaction with OH and the use of γ and k_{rx} to model the reaction gives a time history for the system that matches experiments. As shown in Figure 2, squalane is distributed uniformly within the particle using a reaction-diffusion model, confirming that the system is well-mixed on the timescale of the oxidation chemistry. The difference between the single and multi-compartment models is that in the latter, OH is constrained to interact only with the surface of the particle. Under this physically realistic assumption, squalane molecules not at the surface become available for reaction only through diffusion, which is concentration gradient-driven and not necessarily much faster than the reaction rate. *This indicates that the expression for uptake (Eq. 1) carries an underlying assumption that a well-mixed system is instantaneously mixed.*

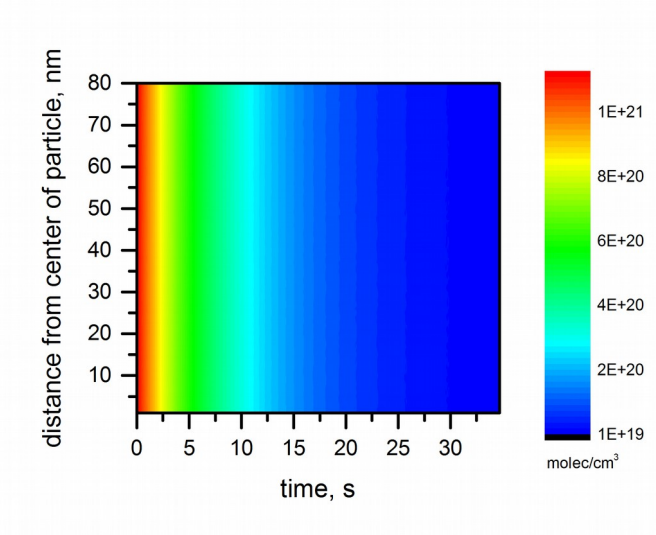

Figure 2. Contour plots connecting the location of reaction events with squalane distribution as a function of time. The concentration scale is molecules/cm^3.

The spatially- and time-resolved reactant and product distributions enable several key aspects of the aerosol particle chemistry to be examined. Plots of the location of the H abstraction and peroxidation (R· + O_2) events are shown in the particle in Figs 3a and 3b, respectively. These event locations are tracked by accumulating markers each time an abstraction or a peroxidation event occurs in a compartment, which can be readily done in stochastic simulations without perturbing the calculations. The prediction that free radical reactions occur to some depth below the surface indicates that although no persistent OH appears in the simulation results, OH can diffuse occasionally to a significant depth in the particle before reacting. Most reactions occur at or very near the surface (within ~5 nm) however. The calculations confirm that although the initial free radical reactions are located primarily at the particle surface, rapid mixing within the particle leads to uniform conversion of squalane as observed experimentally.

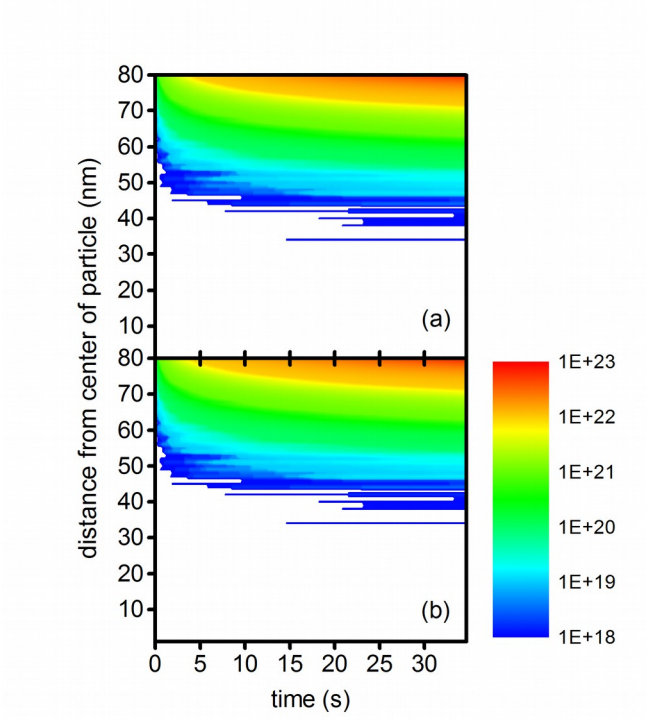

Figure 3. Contour plots showing (a) the location of H abstraction events by OH, cumulative for all generations, and (b) location of the O_2 reaction with newly generated free radicals (R•), cumulative for all generations. The scale is total events/cm^3, presented as logarithmic to reveal rare but significant subsurface events.

Figure 4 shows contour plots of the concentration of the first, second and third generation peroxy radicals. These species are relatively unreactive, and although initially formed near the surface of the particle, are long-lived enough to diffuse uniformly throughout the particle. The steady state peroxy concentration is highest for the first generation, formed from squalane, because it only has one available disproportionation pathway (i.e. reaction with other first generation RO_2·). As second and third generation oxidized peroxy radicals, which are formed by OH reactions with oxidized products of squalane, start to appear, multiple second order reaction pathways are available, and the steady state concentration of total peroxy species drops. The radical and radical reaction event spatial distributions are currently inaccessible experimentally for validation tests, but the successful match of the predicted product distributions to observed data provides some confidence that they are reasonable.

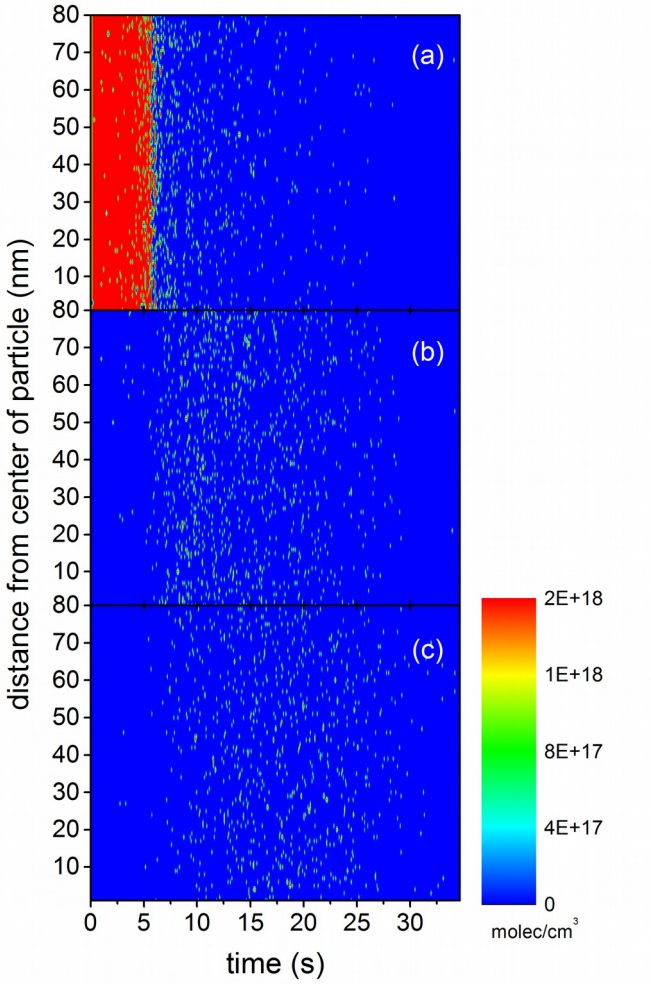

Figure 4. Contour plots showing density of peroxy radicals as a function of time, (a) first (b) second and (c) third generations.

4. Discussion

The simulations, performed with a simple mechanism that quantitatively captures the basic trends in the chemistry, have revealed two key findings: (1) the experimentally determined γ does not represent a sticking or accommodation coefficient for this well-mixed system; and (2) well-mixed does not mean instantaneously mixed. The definition of γ in Eq. 1 has only an apparent chemical rate constant and does not explicitly include transport within the particle, therefore does not fully capture the kinetics controlling the transformation of the aerosol particle.

To reconcile these findings with known features of the uptake process, we consider the current understanding of the underlying physics. In unreactive systems, uptake is treated as an interaction of a gas with a region of reduced density at the surface of the liquid particle, followed by cluster entrapment and merging into the bulk.[58] In reactive systems more complex processes appear to be involved. In a recent discussion,[17] the uptake process is described using coupled reaction-diffusion differential equations, *i.e.* as an inherently kinetic process. The zones where gas uptake occurs are defined, and accommodation is used to describe the gas-to-liquid phase transfer process. The location of a reaction is

determined by the accessible thickness of liquid for the reacting system.[59]

A key question emerges: What determines the accessible liquid thickness for OH reacting with squalane? The simplest measure of this thickness is the reacto-diffusion length calculated using the diffusion coefficient (DOH) for OH in the liquid particle, and its pseudo-first order abstraction rate constant as a time interval Δt_{abs} for the mean distance that OH diffuses prior to reaction, $L_{OH} = \sqrt{D_{OH}\,\Delta t_{|¿|}}$. Using the values for D_{OH}[60] and $|¿| = ¿\,\Delta t_{¿}$ $1/k_{abs}$ (the second order rate constant for H abstraction multiplied by the squalane concentration, 1.14 x 10^{21} molec/cm^3), L_{OH} is << 1 nm. This is not consistent with the definition of γ, experimental observations, or the present single compartment simulation results that show that the entire particle is effectively accessible for reaction.

We postulate that the reacto-diffusion length L in a well-mixed particle is more appropriately defined as $L = \sqrt{2 D_{orgn} \Delta t_{coll}}$, where D_{orgn} is the one-dimensional, radial self-diffusion coefficient of the organic component of the particle, and the time interval is determined by the reactive collision frequency of OH with the particle surface. This is distinct from several other definitions in the literature[22, 24, 61] in an important conceptual way. Relationships have been proposed that utilize the reaction rate constant between the gas molecule and the organic species in the aerosol, whether at the surface or in the bulk, to provide a fundamental clock in the coupled reaction-diffusion system. The reactant from the gas phase is assumed to build up to a finite steady-state concentration in and on the particle, where the rate-determining bimolecular reactions occur. The reacto-diffusion length is determined by how fast the surface organic can be replenished via diffusion from the bulk in between reaction events. The definition we propose here is a more general one that does not depend on the magnitude of the reaction rate constant. Rather, it says that the relevant kinetic clock or reacto-diffusion timescale is the time in between adsorption events, and the organic molecules accessible for reaction are the ones that can potentially reach the newly incident OH during that time interval. If the partial pressure of reactants is low, collisions are rare and the reacto-diffusion length is the entire particle, meaning that any specific organic molecule in the particle has the potential to access and react with the gas species. If the partial pressure is high and the time between collisions is short, only organic molecules close to the surface will be available.

The elementary reactive gas-particle collision frequency is determined by

$$\Delta t_{coll} = \frac{4}{\sigma c \pi D_p^2 n_{OH}} \qquad (5)$$

Substituting Eq. 5 into the expression for L gives

$$L = \left(\frac{8 D_{orgn}}{n_{OH} c \pi D_p^2 \sigma} \right)^{\frac{1}{2}} \qquad (6)$$

For D_{orgn} = 8.5 x 10^{-7}cm^2/s,[47] D_p = 160nm, σ = 1 x 10^{-4} as determined from the simulations, and an OH density of 1 x 10^{11} molec/cm^3, we estimate L is approximately 2000 nm. This value is consistent with the entire squalane particle being available for reaction with an incident OH radical, and that this would hold true up to particle sizes of several microns. Eq 6 contains no specific assumptions about reaction rates or materials types, and we propose that it is a more general way to describe the thickness of the accessible liquid on the particle surface, and in the case of reacting systems, the reacto-diffusion length. An exploration of trends predicted by this expression is presented later in this section.

Taking the standard definition of the uptake coefficient, γ, as given in Eq. 1, and substituting the volume of an accessible shell of thickness L for the particle volume yields

$$\gamma = \frac{2 k_{rx} \rho_0 N_A}{3 c M D_p^2} \left[D_p^3 - (D_p - 2L)^3 \right] \qquad (7)$$

This is a general expression, applicable to viscous and fluid aerosol organics alike, and consistent with discussions in the literature.[1,62] Eq. 7 cannot be connected to microscopic events such as sticking of gases to the particle or subsequent free radical chain reactions that consume the aerosol material. However, by considering the case where the aerosol is well-mixed together with the definition of L in Eq. 6, such a connection can be made.

When the particle is well mixed, the organic aerosol material is sufficiently fluid to move freely throughout the particle in between sticking events. In this case, the volume of the accessible shell is the same size as the volume of the particle, $D_p = 2L$, and by substituting equation (6) into the expression for γ in Eq. 7, we find

$$\gamma = \frac{8 k_{rx} \rho_0 N_A}{3 c M} \left(\frac{2 D_{orgn}}{n_{OH} c \pi D_p^2 \sigma} \right)^{1/2} \qquad (8)$$

This equation, derived for a specific case, provides a means of experimentally determining an elementary sticking probability σ from γ in for aerosol systems in which the particle is sufficiently fluid that the system is well-mixed on the timescale of accommodation or sticking and reaction. By equating equations (1) and (7), and simplifying, we obtain a fundamental relationship between σ and the characteristics of the gas-aerosol system:

$$\sigma = \frac{32 D_{orgn}}{n_{OH} c \pi D_p^4} \qquad (9)$$

Eq. 9 can be rewritten in terms of viscosity using the Stokes-Einstein equation. Since viscosities can be more readily measured than self-diffusion coefficients, this offers a means of predicting values of σ and γ from a broad range

of well-mixed aerosol systems to test the relationships presented here. As will be discussed below, well-mixed is a property that depends on the gas reactant density and particle characteristics, so careful experimental design should enable a great variety of chemical systems to be investigated.

Eq. 9 indicates that an experimentally determined σ has 3 major dependencies: the self-diffusion of the particle's chemical components, the size of the particle, and the partial pressure of the gas phase reactant. This indicates that the underlying physics of the sticking of a gas molecule on the aerosol surface is determined in part by the motion of the organic molecules in between gas collisions, and is therefore an *emergent property of the reacting system* rather than being dictated by the properties of the aerosol material and the interaction potential of it with the gaseous molecule alone. The simulation results are not consistent with a simple kinetic model of gaseous adsorption as would be used for a solid surface. The idea that gas adsorption onto liquids has a significant dependence on molecular motions of the condensed phase species is a key concept but does not say whether liquid motions are important on a microscopic level. There are studies that propose that gas adsorption requires formation of small cavities or rough areas at the liquid surface to facilitate energy transfer and full accommodation,[63-65] and exploration of the role of instantaneous fluctuations in aerosol oxidation would be valuable.

Eq. 8 and 9 obtain for well-mixed systems and can be interpreted in two ways:
(a) σ is not a constant but varies inversely with OH partial pressure and particle size under all conditions. In this case γ is predicted to be always a constant that is characteristic only of the chemical properties of the reacting system; and
(b) σ is a constant determined by the specific properties of the system and can be determined from measurements of γ when the organic particle is well mixed and particle properties are known. In this case γ is expected to vary with particle size, viscosity and reactant partial pressure for a given organic.

There is insufficient information in the present work to evaluate which of these two interpretations is correct. Therefore, we consider recent literature. Measurements of water adsorbed on butanol through the butanol melting point[66] revealed an abrupt increase in water uptake as butanol liquefied. The authors were using water as a probe of the formation of liquid butanol a few degrees below the melting temperature, and elegantly demonstrated its presence. They did not interpret the change in uptake coefficient specifically in this work. We propose that this change in γ is likely to be attributable to a change in the self-diffusion or viscosity of the butanol on melting. In another study,[56] OH uptake for a series of model organic films representative of biomass burning aerosols was measured as a function of [OH] revealing a strong decrease in γ with increasing [OH]. This trend was attributed to formation of a persistent layer of adsorbed species on the surfaces of the particles at higher [OH] that eventually stopped the reaction. We find no accumulation of OH in our simulations, even though this process is allowed up to a depth of 1nm, due to its fast reaction. An alternative interpretation is that the decrease in γ as OH increases is a result of the partial pressure dependence shown in Eq. 8. Finally, a number of recent studies have shown significant changes in the measured reactive uptake coefficient and product formation with aerosol phase (e.g. solid, semisolid, aqueous).[1, 67-69] Taken together, these results provide evidence that γ varies with organic mobility and OH partial pressure, indicating that case b (see above) is most likely to apply: σ is a constant, elementary property of the chemical system, and therefore γ will vary according to the aerosol's reaction conditions.

To consider the atmospheric implications of these results, Eq. 6 was used to predict the diameter of the maximum particle that will behave as if it is well-mixed over a range of self-diffusion coefficients, proportional to the viscosity of the organic species, and OH partial pressures, as shown in Figure 5. This comparison assumes that one underlying chemical reaction mechanism, i.e. OH reaction with an aliphatic organic molecule, is operant across this range of conditions, and would be appropriate for the cases of liquid, semisolid and solid materials having that chemistry. Using OH densities in the range of 1×10^{11} molec/cm^3, particles with self diffusion coefficients spanning 9×10^{-7} (squalane) to 4×10^{-11} cm^2/s (in the low semi-solid range, viscosity of about 1×10^3 Pa-s)[1] and sizes from 50-600 nm are predicted to appear well mixed. Larger squalane-like particles and all particles having higher viscosities will not. Under atmospheric conditions, however, when the OH density is about 1×10^6 molec/cm^3, the well-mixed range expands to include particles as small as 50 nm with self-diffusion coefficients down to 1×10^{-15} cm^2/s, corresponding to a viscosity of more than 10^7 Pa s. This is because collisions leading to sticking and reaction are rare compared to the intrinsic internal mobility timescale. At higher OH densities, however, lower viscosities are required for well-mixed behavior to be observed, and for certain combinations even very small particles will not appear to be well-mixed.

Particles outside of the well-mixed range will appear to be have low uptake coefficients, as illustrated in Figure 6, which shows trends in γ as a function of OH density and particle size calculated for several organic self-diffusion coefficients using Eq 8. The ranges selected for OH density, spanning typical low atmospheric densities to parts per hundred, illustrate how uptake coefficients can vary over a broad range of conditions. In particular, there are regimes where uptake will be invariant with OH density, and where uptake will be very small. When these values for γ are substituted into Equation 1 and size corrections are applied, second order rate coefficients for the overall heterogeneous oxidation rate of aliphatic aerosol particles can be estimated for a range of experimental conditions, and used for predictive purposes in models.

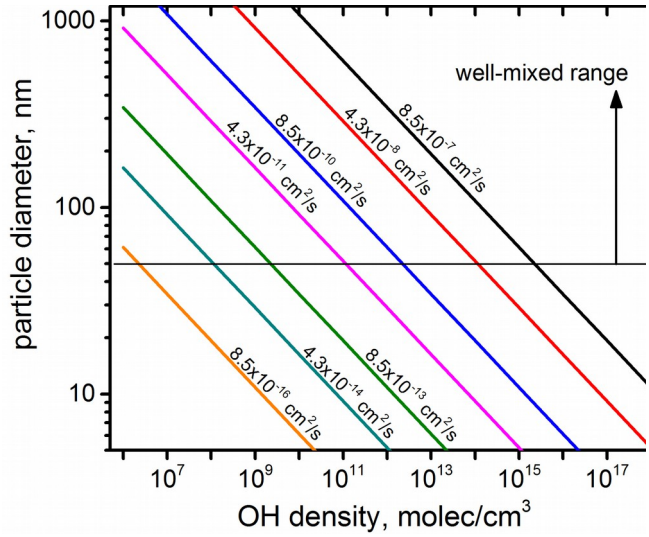

Figure 5. Calculated maximum particle diameters that will react as if well-mixed, as a function of organic self-diffusion coefficient (labeled on each line) and OH density. The criterion of well-mixed is determined using Equation 6 to find conditions where $L > D_p$.

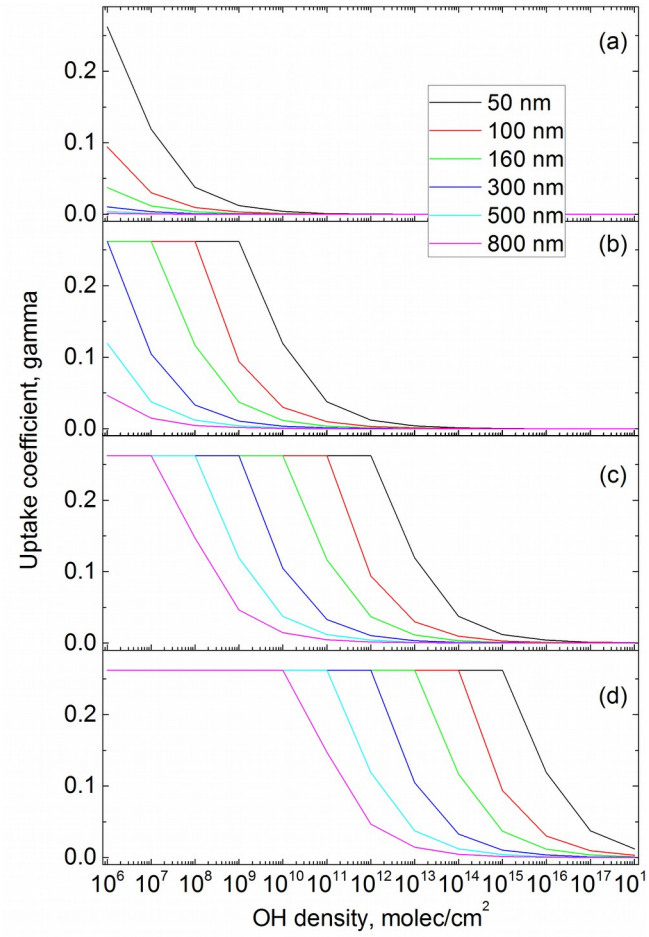

Figure 6. Predicted scaling of γ, whose maximum value is assumed to be 0.26 consistent with the experimental value for squalane under well-mixed conditions, as a function of particle size and OH density assuming a self diffusion coefficient (D_{org}) typical of: (a) squalane, 8.5 x 10^{-7} cm^2/s, (b) a viscous fluid 8.5 x 10^{-10} cm^2/s, (c) a soft semi-solid, 8.5 x 10^{-13} cm^2/s, and (d) a stiff semi-solid, 8.5 x 10^{-16} cm^2/s.

Explicit reaction-diffusion simulations for selected parameter combinations were performed to validate these predictions. Figure 7 presents contour plots for 160 nm particles of squalane for two OH densities and Figure 8 shows analogous plots for a 50 nm particle of a hypothetical squalane-like semi-solid organic material. In both cases it is clear that when γ is > 0.1, the particle behaves as if it is well-mixed independent of its liquid or solid nature because the time in between reactant collisions is sufficient for the required movement. When it is < 0.1 – and more likely close to 0.01 – it is not well mixed. Thus, higher reactant partial pressures will affect the measured uptake coefficients even though the underlying gas-particle reaction mechanism has not changed, in agreement with experimental observations.[56, 66] It is evident that apparent liquid and glassy behaviours as determined from uptake coefficients may be *situational*, and may not reflect the intrinsic chemical state of the aerosol.

While the development of Equations 8 and 9 has involved one class of chemical systems – aliphatic hydrocarbon aerosol launched by free radical abstraction of H – they are more general in form and predict trends consistent with observations in other systems. Quantitative comparisons to other chemical systems require independent knowledge of the aerosol viscosity (for estimation of D_{orgn}), particularly for mixtures, and the sticking coefficient □. The sticking coefficient can be estimated from reaction-diffusion simulations as long as kinetic data for the chemical reactions are known, however viscosity data for a broad range of fluid and semi-solid materials are required to determine the applicability of Equations 8 and 9 and validate the calculations. Comparisons are currently underway in our laboratory using published uptake and transformation measurements as well as new studies of viscosity as a function of reaction conditions, and work by others will also be very valuable. These studies will serve to clarify the range of validity of the equations, and indicate where refinements are needed.

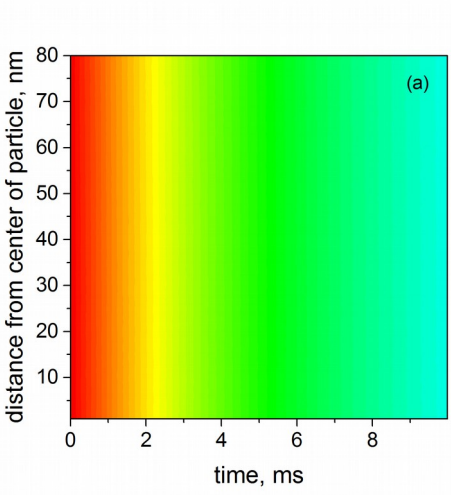

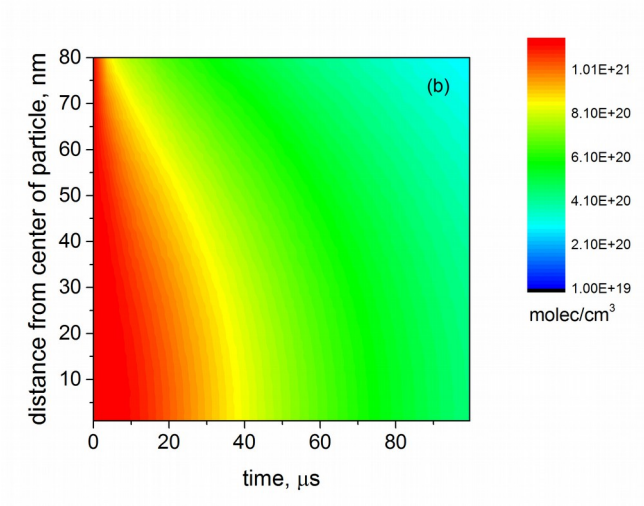

Figure 7. Contour plots for the disappearance of squalane in 160 nm particles as a function of OH partial pressure. (a) [OH] = 1 x 10^{14} molec/cm^3, predicted γ of 0.12, to be compared to Figure 4a; (b) [OH] = 1 x 10^{16} molec/cm^3, predicted γ of 0.01. Concentration units are molec/cm^3.

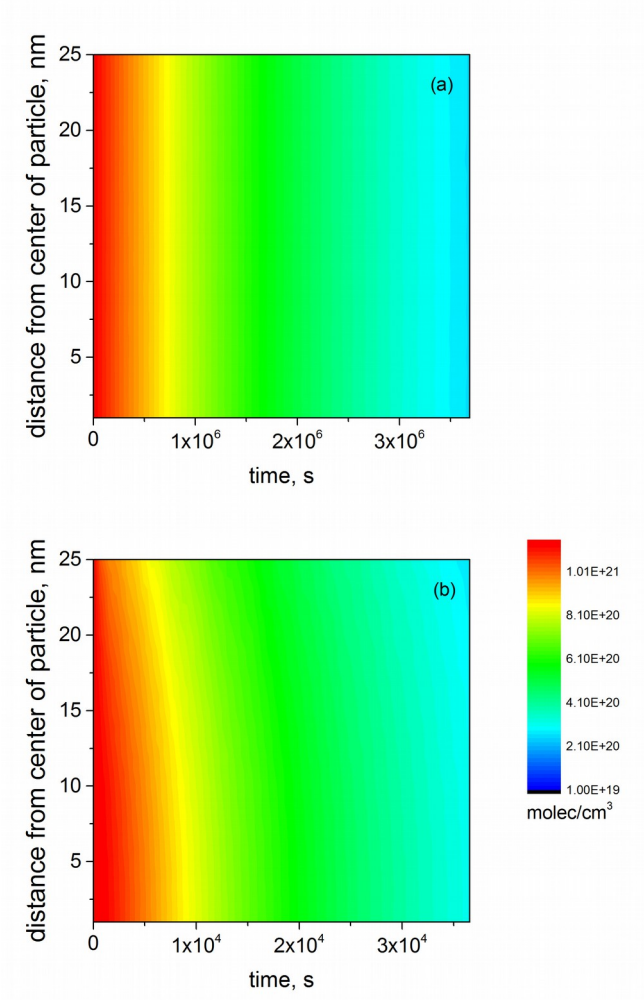

Figure 8. Contour plots for disappearance of aliphatic organics having squalane-like chemistry and a self-diffusion coefficient of 8.5 x 10^{-16} cm^2/s as a function of OH partial pressure. The particle size is 50 nm. (a) [OH] = 1 x 10^6 molec/cm^3, predicted γ of 0.26; (b) [OH] = 1 x 10^8 molec/cm^3, predicted γ of 0.04.

6. Conclusions

We have developed a simple reaction-diffusion model of the reaction of squalane, a model aerosol, with OH radicals to examine reactive uptake in the early stages of the oxidative process. Because the simulations are directly validated using experimental data, they can be used to examine the underlying physical processes. We show that uptake is not equivalent to gas accommodation or sticking in this fast-reacting system. Rather, the magnitude of the uptake coefficient depends in a complex way on both the OH density in the gas phase and the size and materials characteristics of the aerosol particle. Using these results we predict that a particle can have an uptake coefficient typical of a well-mixed liquid system even when it is a semi-solid if the particle is small and OH collisions are rare. This is a result of the dependence of internal diffusion rates on particle size: at the nanoscale composition gradients can become very steep and lead to fast diffusion rates even when the diffusion coefficient is very small. The results of this study indicate that extrapolation of chemical transformation trends from the laboratory to atmospheric conditions should be done with care. A recent paper has examined the equilibration of water within mixed dicarboxylic acid aerosol particles as a function of viscosity and pointed to the need for more refined descriptions of liquid and glassy phases, and their connection to aerosol properties in laboratory and natural environments.[70] Connection of phase properties to reactivity requires consideration of the aerosol and its environment as a whole, and the computational approach described in this work, shown to apply over a very large range of particle sizes and gas partial pressures, may be helpful in doing so.

Acknowledgements

This material is based upon work supported by the Laboratory Directed Research and Development Program of the Department of Energy's Lawrence Berkeley National Laboratory under U.S. Department of Energy Office of Science, Office of Basic Energy Sciences under Contract No. DE-AC02-05CH11231. Results were used from past K.R.W. work supported by the Department of Energy's Office of Science Early Career Research Program and by Chemical Sciences Division of the U.S. Department of Energy under Contract No. DE-AC02-05CH11231. W.D.H. is supported by CHTC. The authors acknowledge Dr. Michael Ward for valuable discussions.

7. Notes and references

*First corresponding author fahoule@lbl.gov , second corresponding author krwilson@lbl.gov

[a] Chemical Sciences Division, Lawrence Berkeley National Laboratory, Berkeley, CA 94720.

[b] Columbia Hill Technical Consulting, Fremont, CA 94539.

1. M. Shiraiwa, M. Ammann, T. Koop and U. Poschl, *Proc. Natl. Acad. Sci. U. S. A.*, 2011, **108**, 11003-11008.

2. J. F. Pankow, *Atmos. Environ.*, 1994, **28**, 189-193.

3. C. D. Cappa and K. R. Wilson, *Atmos. Chem. Phys.*, 2011, **11**, 1895-1911.

4. L. Renbaum-Wolff, J. W. Grayson, A. P. Bateman, M. Kuwata, M. Sellier, B. J. Murray, J. E. Shilling, S. T. Martin and A. K. Bertram, *Proc. Natl. Acad. Sci. U. S. A.*, 2013, **110**, 8014-8019.

5. T. D. Vaden, C. Song, R. A. Zaveri, D. Imre and A. Zelenyuk, *Proc. Natl. Acad. Sci. U. S. A.*, 2010, **107**, 6658-6663.

6. A. Virtanen, J. Joutsensaari, T. Koop, J. Kannosto, P. Yli-Pirila, J. Leskinen, J. M. Makela, J. K. Holopainen, U. Poschl, M. Kulmala, D. R. Worsnop and A. Laaksonen, *Nature*, 2010, **467**, 824-827.

7. D. L. Bones, J. P. Reid, D. M. Lienhard and U. K. Krieger, *Proc. Natl. Acad. Sci. U. S. A.*, 2012, **109**, 11613-11618.

8. A. K. Bertram, A. V. Ivanov, M. Hunter, L. T. Molina and M. J. Molina, *J. Phys. Chem. A*, 2001, **105**, 9415-9421.

9. T. L. Eliason, J. B. Gilman and V. Vaida, *Atmos. Environ.*, 2004, **38**, 1367-1378.

10. I. J. George and J. P. D. Abbatt, *Nat. Chem.*, 2010, **2**, 713-722.

11. J. D. Hearn and G. D. Smith, *Geophys. Res. Lett.*, 2006, **33**, 1-5.

12. G. Isaacman, A. W. H. Chan, T. Nah, D. R. Worton, C. R. Ruehl, K. R. Wilson and A. H. Goldstein, *Environ. Sci. Technol.*, 2012, **46**, 10632-10640.

13. S. H. Kessler, T. Nah, K. E. Daumit, J. D. Smith, S. R. Leone, C. E. Kolb, D. R. Worsnop, K. R. Wilson and J. H. Kroll, *J. Phys. Chem. A*, 2012, **116**, 6358-6365.

14. M. Molina, A. Ivanov, S. Trakhtenberg and L. Molina, *Geophys. Res. Lett.*, 2004, **31**, 1-5.

15. Y. Rudich, N. M. Donahue and T. F. Mentel, *Annu. Rev. Phys. Chem.*, 2007, **58**, 321-352.

16. J. D. Smith, J. H. Kroll, C. D. Cappa, D. L. Che, C. L. Liu, M. Ahmed, S. R. Leone, D. R. Worsnop and K. R. Wilson, *Atmos. Chem. Phys.*, 2009, **9**, 3209-3222.

17. C. E. Kolb, R. A. Cox, J. P. D. Abbatt, M. Ammann, E. J. Davis, D. J. Donaldson, B. C. Garrett, C. George, P. T. Griffiths, D. R. Hanson, M. Kulmala, G. McFiggans, U. Poschl, I. Riipinen, M. J. Rossi, Y. Rudich, P. E. Wagner, P. M. Winkler, D. R. Worsnop and C. D. O' Dowd, *Atmos. Chem. Phys.*, 2010, **10**, 10561-10605.

18. P. A. J. Bagot, C. Waring, M. L. Costen and K. G. McKendrick, *J. Phys. Chem. C*, 2008, **112**, 10868-10877.

19. C.-L. Liu, J. D. Smith, D. L. Che, M. Ahmed, S. R. Leone and K. R. Wilson, *Phys. Chem. Chem. Phys.*, 2011, **13**, 8993-9007.

20. I. J. George, A. Vlasenko, J. G. Slowik, K. Broekhuizen and J. P. D. Abbatt, *Atmos. Chem. Phys.*, 2007, **7**, 4187-4201.

21. A. T. Lambe, J. Y. Zhang, A. M. Sage and N. M. Donahue, *Environ. Sci. Technol.*, 2007, **41**, 2357-2363.

22. D. R. Worsnop, J. W. Morris, Q. Shi, P. Davidovits and C. E. Kolb, *Geophysical Research Letters*, 2002, **29**, 4.

23. M. Shiraiwa, C. Pfrang, T. Koop and U. Poschl, *Atmos. Chem. Phys.*, 2012, **12**, 2777-2794.

24. T. Berkemeier, A. J. Huisman, M. Ammann, M. Shiraiwa, T. Koop and U. Poeschl, *Atmos. Chem. Phys.*, 2013, **13**, 6663-6686.

25. J. Julin, M. Shiraiwa, R. E. H. Miles, J. P. Reid, U. Poschl and I. Riipinen, *Journal of Physical Chemistry A*, 2013, **117**, 410-420.

26. M. Shiraiwa and J. H. Seinfeld, *Geophysical Research Letters*, 2012, **39**.

27. M. Shiraiwa, L. D. Yee, K. A. Schilling, C. L. Loza, J. S. Craven, A. Zuend, P. J. Ziemann and J. H. Seinfeld, *Proc. Natl. Acad. Sci. U. S. A.*, 2013, **110**, 11746-11750.

28. M. Shiraiwa, A. Zuend, A. K. Bertram and J. H. Seinfeld, *Physical Chemistry Chemical Physics*, 2013, **15**, 11441-11453.

29. S. Zhou, M. Shiraiwa, R. D. McWhinney, U. Poeschl and J. P. D. Abbatt, *Faraday Discussions*, 2013, **165**, 391-406.

30. J. H. Kroll, J. D. Smith, D. L. Che, S. H. Kessler, D. R. Worsnop and K. R. Wilson, *Physical Chemistry Chemical Physics*, 2009, **11**, 8005-8014.

31. K. R. Wilson, J. D. Smith, S. H. Kessler and J. H. Kroll, *Phys. Chem. Chem. Phys.*, 2012, **14**, 1468-1479.

32. C. R. Ruehl, T. Nah, G. Isaacman, D. R. Worton, A. W. H. Chan, K. R. Kolesar, C. D. Cappa, A. H. Goldstein and K. R. Wilson, *Journal of Physical Chemistry A*, 2013, **117**, 3990-4000.

33. W. D. Hinsberg and F. A. Houle.

34. D. L. Bunker, B. Garrett, T. Kleindienst and G. S. Long, *Combust. Flame*, 1974, **23**, 373-379.

35. D. T. Gillespie, *J. Comput. Phys.*, 1976, **22**, 403-434.

36. D. T. Gillespie, *J. Chem. Phys.*, 2001, **115**, 1716-1733.

37. W. Hinsberg and F. A. Houle, *U. S. Patent No. 5625579 (April 29, 1997)*, 1997.

38. W. Hinsberg and F. A. Houle, *U. S. Patent No. 5826065 (October 20, 1998)*, 1998.

39. F. A. Houle, W. D. Hinsberg, M. Morrison, M. I. Sanchez, G. Wallraff, C. Larson and J. Hoffnagle, *Journal of Vacuum Science and Technology B*, 2000, **18**, 1874-1885.

40. F. A. Houle and W. D. Hinsberg, *J. Phys. Chem.*, 1995, **99**, 14477-14485.

41. F. A. Houle, W. D. Hinsberg and M. I. Sanchez, *Macromolecules*, 2002, **35**, 8591-8600.

42. A. A. W. Wiegel, K. R.; Hinsberg, W. D.; Houle, F. A. (unpublished work).

43. G. A. Russell, *J. Am. Chem. Soc.*, 1957, **79**, 3871-3877.

44. J. E. Bennett and R. Summers, *Can. J. Chem.-Rev. Can. Chim.*, 1974, **52**, 1377-1379.

45. R. Atkinson, *Atmos. Chem. Phys.*, 2003, **3**, 2233-2307.

46. E. T. Denisov and I. B. Afanas'ev, *Oxidation and Antioxidants in Organic Chemistry and Biology*, Taylor & Francis, 2005.

47. E. von Meerwall, S. Beckman, J. Jang and W. L. Mattice, *J. Chem. Phys.*, 1998, **108**, 4299-4304.

48. A. J. Easteal, *J. Chem. Eng. Data*, 1996, **41**, 741-744.

49. S. V. Vasenkov, V. A. Bagryansky, V. V. Korolev and V. A. Tolkatchev, *Radiat. Phys. Chem.*, 1991, **38**, 191-197.

50. C. W. Harmon, C. R. Ruehl, C. D. Cappa and K. R. Wilson, *Physical Chemistry Chemical Physics*, 2013, **15**, 9679-9693.

51. V. F. McNeill, R. L. N. Yatavelli, J. A. Thornton, C. B. Stipe and O. Landgrebe, *Atmos. Chem. Phys.*, 2008, **8**, 5465-5476.

52. M. J. P. Comunas, X. Paredes, F. M. Gacino, J. Fernandez, J. P. Bazile, C. Boned, J. L. Daridon, G. Galliero, J. Pauly, K. R. Harris, M. J. Assael and S. K. Mylona, *J Phys Chem Ref Data*, 2013, **42**.

53. C. Waring, K. L. King, P. A. J. Bagot, M. L. Costen and K. G. McKendrick, *Physical Chemistry Chemical Physics*, 2011, **13**, 8457-8469.

54. S. Enami, M. R. Hoffmann and A. J. Colussi, *The journal of physical chemistry. A*, 2014, **118**, 4130-4137.

55. T. Moise and Y. Rudich, *Geophysical Research Letters*, 2001, **28**, 4083-4086.

56. J. H. Slade and D. A. Knopf, *Physical Chemistry Chemical Physics*, 2013, **15**, 5898-5915.

57. P. L. Cooper and J. P. D. Abbatt, *J. Phys. Chem.*, 1996, **100**, 2249-2254.

58. P. Davidovits, J. H. Hu, D. R. Worsnop, M. S. Zahniser and C. E. Kolb, *Faraday Discussions*, 1995, **100**, 65-81.

59. P. Davidovits, C. E. Kolb, L. R. Williams, J. T. Jayne and D. R. Worsnop, *Chem. Rev.*, 2011, **111**, PR76-PR109.

60. J. T. Su, P. B. Duncan, A. Momaya, A. Jutila and D. Needham, *J. Chem. Phys.*, 2010, **132**, -.

61. G. D. Smith, E. Woods, T. Baer and R. E. Miller, *Journal of Physical Chemistry A*, 2003, **107**, 9582-9587.

62. C. Pfrang, M. Shiraiwa and U. Poschl, *Atmos. Chem. Phys.*, 2011, **11**, 7343-7354.

63. M. E. King, M. E. Saecker and G. M. Nathanson, *J. Chem. Phys.*, 1994, **101**, 2539-2547.

64. G. M. Nathanson, *Annu. Rev. Phys. Chem.*, 2004, **55**, 231-255.

65. G. L. Pollack, *Science*, 1991, **251**, 1323-1330.

66. P. Papagiannakopoulos, X. R. Kong, E. S. Thomson, N. Markovic and J. B. C. Pettersson, *J. Phys. Chem. C*, 2013, **117**, 6678-6685.

67. F. D. Pope, P. J. Gallimore, S. J. Fuller, R. A. Cox and M. Kalberer, *Environmental Science & Technology*, 2010, **44**, 6656-6660.

68. M. N. Chan, H. Zhang, A. H. Goldstein and K. R. Wilson, *J. Phys. Chem. C*, 2014, **10.1021/jp5012022**.

69. L. H. Renbaum and G. D. Smith, *Physical Chemistry Chemical Physics*, 2009, **11**, 2441-2451.

70. A. M. Booth, B. Murphy, I. Riipinen, C. J. Percival and D. O. Topping, *Environmental Science & Technology*, 2014.